DOI: 10.1002/chem.200601013

Reversible Assembly and Disassembly of Gold Nanoparticles Directed by a Zwitterionic Polymer

Ya Ding,[a] Xing-Hua Xia,*[a] and He-Sheng Zhai*[b]

Abstract: Herein, we have successfully introduced the stimuli-response concept into the controllable synthesis of gold nanoparticles (AuNPs) with designed properties. We used a pH-responsive zwitterionic polymer that acted as a template and a stabilizer. Gold colloids prepared in situ from the polymer solution have a narrow size distribution of about 5 nm. The assembly and disassembly of AuNPs can be finely tuned by modulating the net charges of the zwitterionic polymer so that they are either positive or negative as a function of the solution pH. Different aggregates and colors appear on altering the solution pH. In acidic solutions, gold colloids form large symmetrical aggregates, while the AuNPs disperse in solutions with a pH $\approx$ 9.6. However, as the solution pH increases ($>$9.6), needle-like aggregates with a small interparticle distances are formed. On the basis of TEM, SEM, ^{1}H NMR and UV/Vis measurements, we attribute pH-triggered aggregation and color changes of the gold colloids to the ionization process and conformational change of the polymer. The ionization process governs the choice of ligand anchored on the surface of AuNPs, and the conformational change of the polymer modulates the interspaces between AuNPs. The present approach, which is based on a rational design of the physicochemical properties of the template used in the synthesis process, provides a powerful means to control the properties of the nanomaterial. Furthermore, the colorimetric readout can be visualized and applied to future studies on nanoscale switches and sensors.

Keywords: gold · nanoparticles · polymers · self-assembly

Introduction

The study of smart materials that are responsive to a variety of external stimuli, such as pH, ionic strength, temperature, light, magnetic field, or specific biological moieties, is one of the most important areas of materials research, particularly with regards to practical applications.[1] The implementation of such an environmentally responsive process in nanoscience and nanoengineering, namely, the controllable synthesis of materials with designed properties on the nanoscale, can be expected to produce novel materials with a superior structure and function.

[a] Dr. Y. Ding, Prof. X.-H. Xia
Key Laboratory of Analytical Chemistry for Life Science
School of Chemistry and Chemical Engineering
Nanjing University, Nanjing, 210093 (China)
Fax: (+86)258-3597436
E-mail: xhxia@nju.edu.cn

[b] Prof. H.-S. Zhai
Center for Scanning Electron Microscopy
Xiamen University, Xiamen, 361005 (China)
Fax: (+86)592-2188296
E-mail: hszhai@xmu.edu.cn

Up to now, a variety of biomolecules,[2] copolymers,[3] carbohydrates,[4] and other compounds with functional ligands[5] have been employed as templates for assembling nanostructures by means of electrostatic adsorption, covalent binding, and specific affinity interactions.[6,7] These systems provide a toolkit for growing and organizing metallic nanoparticles (NPs) and semiconductor quantum dots. One-dimensional nanostructures, as well as structures with two-dimensional and three-dimension ordering in solutions and on substrate surfaces have been reported.[7]

To successfully introduce the stimuli-response concept into the controllable synthesis of nanomaterials, templates for nanoparticle nucleation and growth should be precisely tailored. A recent example is the development of a colorimetric Pb^{2+} sensor, which functions by the disassembly of gold nanoparticle aggregates controlled by the Pb^{2+}-dependent DNAzyme using DNA as a template.[8] Although periodic sequenced DNA can be engineered in a controlled fashion into heteropolymeric structures, variation of the base, sugar, and phosphate functionalities as well as the DNA sequence makes fine control of the nanomaterials difficult. Other biomolecules with natural repeating units can also be used as programmable templates to assemble materi-

als in a controlled fashion. Among them, chitosan (CS) has homogeneous D-glucosamine units that provide a perfect periodic structure for the design and synthesis of artificial stimuli-responsive templates for nano-objects. Zwitterionic structures are particularly attractive for the fabrication of ligand systems to direct nanoparticle growth. Amino acids, one of the simplest zwitterionic templates, possess both α-amino and carboxyl groups. A previous report has shown that capping of gold NPs with lysine and aspartic acid renders gold NPs water-dispersible, and the interspaces between particles can be changed by protonation of the amino stabilizer at different pH values.[9] However, the morphological change of gold nanoparticle aggregates does not occur in these small molecule template systems. Owing to the unequal number of cation and anion groups in these basic and acidic amino acids, aggregation of gold colloids can occur either in acidic or in basic solutions ($pI_{lysine} \approx 9.4$ and $pI_{aspartic\ acid} \approx 2.77$).[9]

Herein, for the controllable synthesis of nanomaterials, we designed a water-soluble zwitterionic chitosan derivative, 6-*O*-carboxylmethyl chitosan (CMC),[10] in which the degree of substitution of carboxymethyl groups is about 1. It has approximately equal numbers of cationic ($-NH_3^+$) and anionic ($-COO^-$) groups in each D-glucosamine unit along the long chain of chitosan. Gold nanoparticles (AuNPs) were prepared by $NaBH_4$ reduction[11] in the presence of CMC. The amino acid like long-chain structure of CMC then acts as a pH-sensitive template for the reversible assembly and disassembly of AuNPs through the choice of ligands and the conformation changes of the polymer. In contrast to results reported in the literature on the amino acid template approach, the aggregation of AuNPs occurs at both extreme pH values (pH 2.0 and 12.0), resulting in aggregates with completely different shapes. The present approach provides a powerful means for rationally controlling nanoparticle properties. In addition, the colorimetric readout can be seen with the naked eye, providing a sensitive and efficient probe to study conformational changes of macromolecules and biomolecules exposed to various environmental stimuli.

Results and Discussion

Figure 1 shows the transmission electron microscopy (TEM) and selected-area electron diffraction (SAED) images of CMC-stabilized AuNPs at different pH values. At pH 9.6, the AuNPs disperse well in solution. Their average diameter is about 5 nm, as calculated by counting 100 particles in the TEM image (Figure 1a). High-resolution TEM (HRTEM) images of this sample in Figure 1b show that the AuNPs have a spherical morphology. The particle–particle distance is relatively large, ranging from several to tens of nanometers. For an individual gold nanoparticle (see insert in Figure 1b), the distance between two adjacent planes is 0.24 nm, resulting from a group of (111) planes in the face-centered cubic (fcc) structure of Au^0. The electron diffraction pattern of this particle is shown in Figure 1c. As expected, it exhibits a well-defined array of sharp spots, indicating a single crystal rather than rings that would be expected from a polycrystalline sample. When the solution pH is adjusted to a high value (pH 12.0), dispersed AuNPs are clustered into needle-like aggregates (Figure 1d). The HRTEM image shows that these aggregates consist of the clustered AuNPs with a shorter particle–particle distance of less than 3 nm (Figure 1e). Its SAED pattern also exhibits spots that are characteristic of a single crystal (Figure 1f), which confirms that the structure of the aggregates consists of isolated AuNPs. On the contrary, in acidic solution (e.g. pH 2.0), gold aggregates become much larger and denser than those observed at pH 12.0. Gold aggregates are produced with a more regular morphology: about 360 nm long and about 150 nm wide (Figure 1g), with symmetrical angles on both ends of the clusters. Large angular aggregates as the main product can

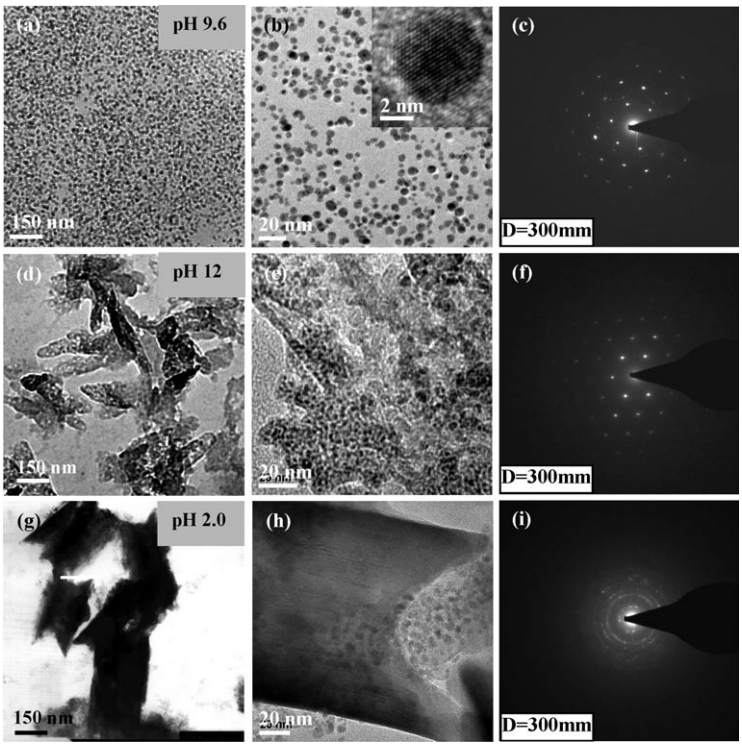

Figure 1. TEM images and SAED patterns of CMC–AuNPs at pH 9.6 (a, b, c), pH 12.0 (d, e, f), and pH 2.0 (g, h, i). Inset (image b): an individual gold nanoparticle.

be observed in the HRTEM image (Figure 1h), which indicates complete fusion of the AuNPs. The SAED image (Figure 1i) exhibits a different pattern with broad halos attributed to the polymeric matrix and sharp rings from a highly crystalline gold nanostructure. In addition, nanoparticles with a shorter particle–particle distance scatter near the main aggregates.

As the solution pH changes, the gold colloid solutions change color, from purple (pH 2.0) to pink (pH 9.6) to mauve (pH 12.0) (see Figure 5). This phenomenon can be described by using the Mie scattering theory:[12] localized surface plasmon resonance (LSPR) arising from interparticle interactions. The color changes associated with the aggregation of metal nanoparticles are attributed to the changes in the particle–particle distance, which was proved by TEM analysis. As expected, in the case of the nanoparticle solution in the absence of CMC, no color change was observed as the solution pH was altered. Therefore, a possible mechanism for tuning nanoparticle interspaces may involve the unique chemical structure and ionization process of CMC (Scheme 1). We find that each glucosamine subunit of

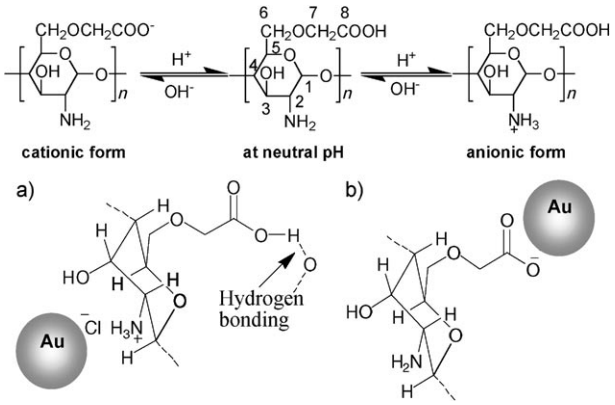

Scheme 1. Chemical structure and ionization of CMC (top), and the change in the chelation mode to AuNP as a function of the pH: a) acidic pH and b) basic pH.

CMC has a pair of acid–base groups: the C2 amino group on the saccharide ring and the carboxyl group attached to the 7-position of the C atom. This amino acid like subunit structure can donate or accept a proton in a basic or an acidic medium, respectively. In acidic solutions, both groups are fully protonated. C2-$NH_3^+Cl^-$ groups are hydrophilic, and thus they can bind to the metallic nanoparticles through the formation of surface ion pairs,[13] with the Cl^- ion attached to the Au surface (Scheme 1a, below). In contrast, carboxylic acid groups facilitate interparticle interactions through both hydrogen bonding and the increase in hydrophobicity, resulting in the formation of particle aggregates (Figure 1g and h). However, as the solution pH increases, the carboxyl and the amino groups will subsequently lose a proton. On the one hand, in solutions with an extremely high pH, C2-NH_3^+ is transformed into the neutral and insoluble C2-NH_2 group, which forms the core of aggregates. On the other hand, particle aggregation is unfavorable owing to the repulsive interactions between the negatively charged carboxylate particles (Scheme 1b, below).[14] Based on the balance of these two driving forces, discrete AuNPs with a shorter particle–particle distance can be explained (Figure 1d and e). At pH 9.6, the existence of functional groups (both -$NH_3^+Cl^-$ and -COO^-) allows the free extension of the long polymer chain, resulting in well-dispersed AuNPs (Figure 1a and b). Thus, either the -$NH_3^+Cl^-$ or the -COO^- ligand from the ionization of CMC plays a crucial role in stabilizing AuNPs and directing aggregation. The exchange of ligands upon altering the pH provides a powerful means of rationally controlling assembly and disassembly of inorganic NPs, which is particularly relevant because the spatial orientation and arrangement of the NPs induced by stimuli-responsive macromolecules are important in the realization of technologically useful nanoparticle-based materials.

To confirm the role of either the -$NH_3^+Cl^-$ or the -COO^- ligand in stabilizing AuNPs, ^{1}H NMR spectra (D_2O) of the polymer–nanoparticle hybrid system were measured under acidic (pH≈2) and basic (pH≈12) conditions (Figure 2). To

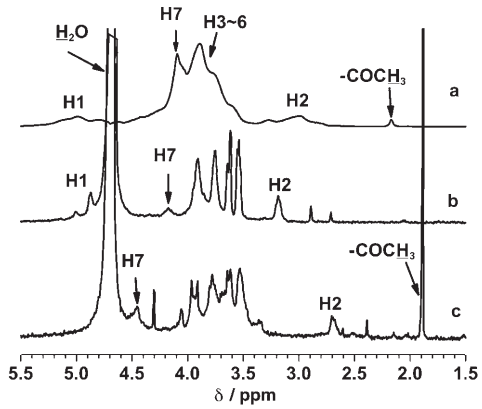

Figure 2. ^{1}H NMR spectra in D_2O: a) CMC at pH 7.0, b) CMC–AuNPs at pH 2.0, and c) CMC-AuNPs at pH 12.0.

make a meaningful comparison, the NMR spectrum of pure CMC at neutral pH (≈7) is also presented in Figure 2 (curve a). The broad proton peaks for pure CMC (curve a) are attributed to the strong hydrogen bonding between saccharide units in CMC.[16] It has been reported that the presence of gold NPs leads to broadening of the proton peaks owing to the effect of the metallic center on the ligands and the "solid-like" nature of the functional groups.[15] However, we found that the peaks in the case of the CMC-AuNPs composite (curves b and c) became much sharper. And the one broad peak for H3–H6 in CMC is split into four sharp peaks. This phenomenon occurs in the whole solution pH range, indicating the decreasing effects of gold NPs on the hydrogen bonding in CMC.

In addition to peak sharpening, pH-dependent shifts of the peak positions were observed. For the CMC-AuNP sample at acidic pH, the signal of H2 is deshielded ($\delta =$

3.19 ppm, curve b) compared to pure CMC at a neutral pH ($\delta = 2.99$ ppm, curve a). This positive shift may be attributable to the effect of the metallic center on the proton peak of C2 next to the $-NH_3^+Cl^-$ ligand (Scheme 1a), which is consistent with our earlier studies on *N*,*N*,*N*-trimethyl chitosan chloride protected gold nanoparticles.[17] In basic solutions, however, the loss of a hydrogen atom from the carboxyl group, which then acts as a ligand to the gold NPs (Scheme 1b), is supported by the change in chemical shifts: the previous signal at $\delta = 4.10$ ppm (H7, curve a; Figure 2) now appears downfield at $\delta = 4.46$ ppm (curve c); a negative shift of the signal H2 from $\delta = 2.99$ to 2.70 ppm is observed; H1 peaks between $\delta = 4.8$ and 5.7 ppm almost disappear, which may be shielded and overlapped by the signal of the strong peak of water.

The SEM images shown in Figure 3 not only display a comparable result for the assembly and disassembly of gold NPs as indicated by the TEM analysis, but also provide more evidence for the morphology of the hybrid polymer–NP aggregates at different pH values. At pH 9.6, the CMC-AuNP complex appears to be loosely dispersed clusters (Figure 3a) of a larger size than the gold NPs in the TEM image, which indicates that CMC acts as a stabilizing layer around the gold particles. The SEM image of a pH 12.0 solution (Figure 3b) also presents a comparable increase in the size of the needle-like gold aggregates. However, the SEM image shows massive aggregates at pH 2.0, which can be attributed to hydrogen bonding among carboxylic acid groups under the acidic conditions discussed above. This hydrogen-bonding effect embeds the gold NP assemblies in the polymer matrix and makes them invisible in the SEM image (Figure 3c).

Color switches of the gold colloid solutions are reversible upon altering the pH. This reversible phenomenon of the pH-driven optical changes for the CMC–gold colloid solution was studied by UV/Vis absorption spectroscopy. The shift of the maximum absorbance wavelength (λ_{max}) in the UV spectra indicates that the changes are completely reversible (Figure 4A). Starting from a solution pH of 9.6 (with the Au plasmon resonance band at 510 nm), the Au plasmon resonance band shifts to 526 nm at pH 2.0 and returns to 515 nm at pH 12.0. However, the intensity of the absorption bands continuously decreases (Figure 4B), particularly during the adjustment from a basic to an acidic medium. In addition, a shoulder at 890 nm is observed in all samples at pH 2.0. As we already know, a red shift in the color of a gold nanoparticle solution can be attributed to new absorp-

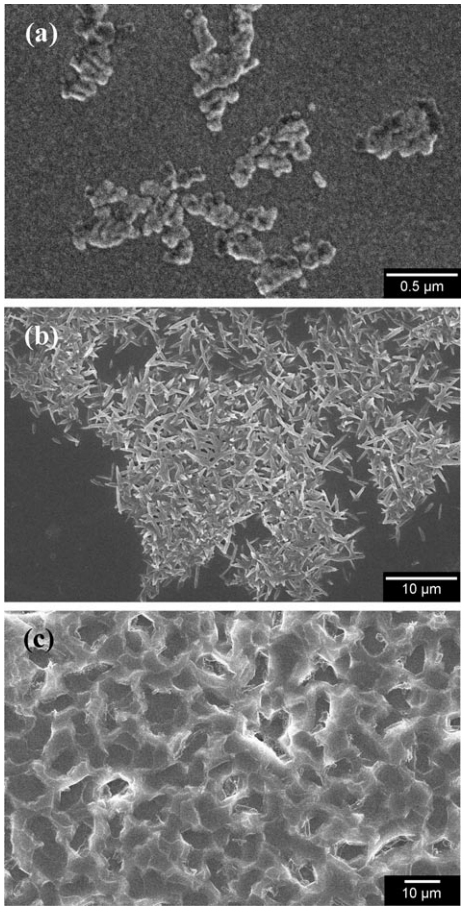

Figure 3. SEM images of CMC-AuNPs at a) pH 9.6, b) pH 12.0, and, c) pH 2.0.

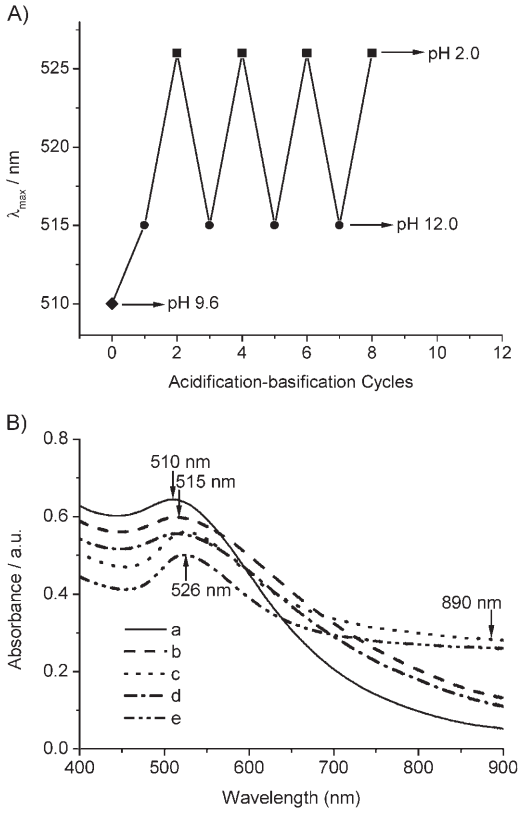

Figure 4. Au plasmon resonance band from an initially pink portion at 510 nm with pH 9.6. A) The solution switches reversibly from a mauve solution (with normal Au plasmon resonance band at 515 nm) to a purple solution (Au plasmon resonance band at 526 nm) between pH 12.0 (●) and pH 2.0 (■). B) UV-visible spectra of the CMC–AuNP solutions at pH: a) 9.6, b) 12.0, c) 2.0, d) 12.0, and e) 2.0 sequentially corresponding to the first five points in (A).

tion bands in the extinction spectrum at long wavelengths. This shoulder is caused by the electric dipole–dipole interaction and by coupling between plasmons of neighboring particles inside the aggregates.[14] For the prepared CMC–gold nanoparticle solutions, the red shift of the absorption peak and the appearance of the shoulder at long wavelengths as a function of the pH value can be attributed to aggregation phenomena of the gold nanoparticles.

To understand the decreasing intensity in the reversibility experiments, the pH of the CMC–gold NP solution was varied from 2.0 to 13.3 by dropwise addition of HCl or NaOH solution. The optical properties of the nanoparticle solution were analyzed by UV/Vis spectroscopy. Figure 5A shows the visual evidence for the effect of pH on the nanoparticle solutions. At pH≈6, the particles are completely precipitated in a short time. This can be explained by the appearance of an isoelectric point (pI) of CMC. At this pH value, the zwitterionic polymer has no net charge, resulting in the lowest solubility of CMC and subsequently in the rapid precipitation of gold NPs. Thus, the UV/Vis absorbance disappears at this point, and the intensity decrease of the UV/Vis spectra in the reversibility experiments can be partly attributed to irreversible processes when the pH value experiences the isoelectric point at pH≈6. Beyond this pH, the CMC–particle complex exhibits a different degree of red shift in the color. λ_{max} shifts (Figure 5B) in the UV spectra indicate regular changes in accordance with the solution color, ranging from 501 nm to 538 nm, except at pH 5.0 and 7.0. At these two points, a sharp absorbance band at 537 nm and a shoulder at 890 nm are observed, similar to the situation in the CMC–gold NP solution at pH 2.0, which can be attributed to the existence of the gold aggregates in solution.

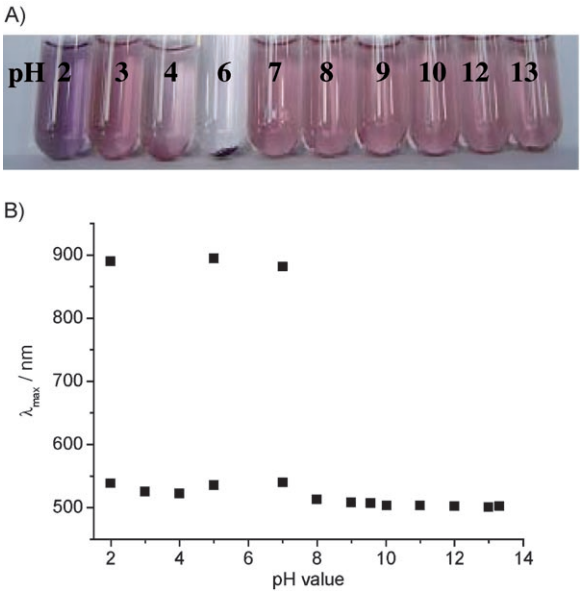

Figure 5. A) Photograph of the CMC–AuNP solutions from pH 2 to pH 13. B) The average maximum absorbance wavelength (λ_{max}) of the AuNP solution at pH 2–14 ($n=3$).

Conclusion

In summary, we report, for the first time, on the control of reversible assembly and disassembly of gold nanoparticles by the use of a well-designed zwitterionic polymer as the template and stabilizer. Simple adjustment of the solution pH led to drastic changes in the aggregate morphologies of these discrete gold nanoparticles. This pH-triggered assembly process of the nanoparticles results from the chosen ligands and conformational changes of the pH-sensitive polymer. A better understanding of the possible mechanism relating to the ionization process and the conformational changes in the zwitterionic polymer at molecular scale should allow further improvements in the rational design of the ideal template used to control NP aggregation, morphology, and properties. In addition, the colorimetric readout can be visualized and used as a probe for studying the conformational changes of macromolecules and biomolecules exposed to various environmental stimuli.

Experimental Section

Materials: Chitosan had a deacetylation degree of 99.5% and polymer-viscosity average molecular weight of 26500 D. All commercially available solvents and reagents were used without further purification.

Synthesis of 6-*O*-CMC: Chitosan (2.0 g, 12.4 mM) was added to an aqueous NaOH solution (10.0 gm, 50 wt%), and the mixture was placed in a refrigerator at −20°C. Alkali chitosan and isopropyl alcohol (20.0 mL) were added to a 100-mL reactor and stirred for 1 h at 40°C. A solution of chloroacetic acid (3.0 g, 31.7 mM) in 2-propanol (20.0 mL) was added dropwise, and the mixture was refluxed for 2 h at 65°C. The resultant solution was adjusted to pH 7.0, and the mixture was dialyzed against deionized water for five days (MWCO 10000). The mixture was lyophilized to afford 1.2 g of the light yellow and water-soluble product. The degree of substitution is controlled in the range of 1.0–1.1, as calculated by the elemental analysis results.

Preparation of CMC-gold nanoparticles: The preparation of CMC-derived materials was carried out in a single-phase system of filtrated sub-boiling water through a microporous membrane with an aperture of 0.22 μm. All glassware was cleaned in a bath of freshly prepared aqua regia (HCl/HNO_3 3:1) and then rinsed thoroughly with deionized water prior to use. An aqueous solution of $HAuCl_4$ (206 μL, 60 mM) was mixed with a diluted solution of CMC (36 mL, 2.2 mg, $AuCl_4^-$/saccharide unit of CMC ratios were 1:1) with vigorous stirring in an ice/water bath for 30 min. A freshly prepared and cooled aqueous solution of $NaBH_4$ (1.2 mL, 0.1 M) was added to the reaction solution, and the color immediately changed to light orange. The solution was stirred for 2 h to afford a pink colloidal dispersion of gold.

The solution of the prepared nanoparticles with pH≈9.6 (because of excess $NaBH_4$) was divided into several portions. Portions of the prepared solution were basified to pH 12.0 with a NaOH solution and acidified to pH 2.0 with a HCl solution.

Characterization: A single drop of each solution was deposited on a TEM grid and then dried in air. All samples of the CMC–AuNPs were measured with a JEM-200CX TEM and JEM-2010 instrument (JEM-100s JEOL, Japan) at an acceleration voltage of 200 kV, and a JSM-6360 LV SEM (JEOL, Japan) at an acceleration voltage of 25 kV. ^{1}H NMR spectra were recorded on a Bruker (AVACE) AV-500 spectrometer. UV/Vis spectra were recorded on a UV-2401 PC UV/Vis spectrophotometer (Shimadzu, USA).

Acknowledgements

This work was supported by grants from the National Natural Science Foundation of China (NSFC, No. 20375016, 20535010) and the National Science Fund for Creative Research Groups (20521503).

[1] a) N. Nath, A. Chilkoti, *Adv. Mater.* **2002**, *14*, 1243–1247; b) S. A. Sukhishvli, *Curr. Opin. Colloid Interface Sci.* **2005**, *10*, 37–44; c) J. Du, S. P. Armes, *J. Am. Chem. Soc.* **2005**, *127*, 12800–12801.

[2] a) H. Yan, S. H. Park, G. Finkelstein, J. H. Reif, T. H. LaBean, *Science* **2003**, *301*, 1882–1884; b) R. Bhattacharya, C. R. Patra, S. Wang, L. Lu, M. J. Yaszemski, D. Mukhopadhyay, P. Mukherjee, *Adv. Funct. Mater.* **2006**, *16*, 395–400; c) C. B. Mao, D. J. Solis, B. D. Reiss, S. T. Kottmann, R. Y. Sweeney, A. Hayhurst, G. Georgiou, B. Iverson, A. M. Belcher, *Science* **2004**, *303*, 213–217.

[3] a) T. Teranishi, I. Kiyokawa, M. Miyake, *Adv. Mater.* **1998**, *10*, 596–599; b) M. K. Corbierre, N. S. Cameron, M. Sutton, S. G. J. Mochrie, L. B. Lurio, A. Rühm, R. B. Lennox, *J. Am. Chem. Soc.* **2001**, *123*, 10411–10412; c) C. H. Walker, J. V. St. John, P. Wisian-Neilson, *J. Am. Chem. Soc.* **2001**, *123*, 3846–3847; d) K. S. Mayya, B. Schoeler, F. Caruso, *Adv. Funct. Mater.* **2003**, *13*, 183–188; e) Y. J. Kang, T. A. Taton, *Angew. Chem.* **2005**, *117*, 413–416; *Angew. Chem. Int. Ed.* **2005**, *44*, 409–412.

[4] a) A. Yoshizumi, N. Kanayama, Y. Maehara, M. Ide, H. Kitano, *Langmuir* **1999**, *15*, 482–488; b) J. M. de la Fuente, A. G. Barrientos, T. C. Rojas, J. Rojo, J. Cañada, A. Fernández, S. Penadés, *Angew. Chem.* **2001**, *113*, 2317–2321; *Angew. Chem. Int. Ed.* **2001**, *40*, 2258–2261; c) H. Otsuka, Y. Akiyama, Y. Nagasaki, K. Kataoka, *J. Am. Chem. Soc.* **2001**, *123*, 8226–8230; d) M. J. Hernáiz, J. M. de la Fuente, Á. G. Barrientos, S. Penadés, *Angew. Chem.* **2002**, *114*, 1624–1627; *Angew. Chem. Int. Ed.* **2002**, *41*, 1554–1557.

[5] a) J. Li, J. Wang, V. G. Gavalas, D. A. Atwood, L. G. Bachas, *Nano Lett.* **2003**, *3*, 55–58; b) A. Schroedter, H. Weller, *Angew. Chem.* **2002**, *114*, 3346–3350; *Angew. Chem. Int. Ed.* **2002**, *41*, 3218–3221; c) K. Naka, H. Itoh, Y. Tampo, Y. Chujo, *Langmuir* **2003**, *19*, 5546–5549; d) O. Abed, A. Vaskevich, R. Arad-Yellin, A. Shanzer, I. Rubinstein, *Chem. Eur. J.* **2005**, *11*, 2836–2841.

[6] a) A. Badia, S. Singh, L. Demers, L. Cuccia, G. R. Brown, R. B. Lennox, *Chem. Eur. J.* **1996**, *2*, 359–363; b) Y. Yamanoi, N. Shirahata, T. Yonezawa, N. Terasaki, N. Yamamoto, Y. Matsui, K. Nishio, H. Masuda, Y. Ikuhara, H. Nishihara, *Chem. Eur. J.* **2006**, *12*, 314–323; W. Huang, G. Masuda, S. Maeda, H. Tanaka, T. Ogawa, *Chem. Eur. J.* **2006**, *12*, 607–619.

[7] M. C. Daniel, D. Astruc, *Chem. Rev.* **2004**, *104*, 293–346.

[8] J. Liu, Y. Lu, *J. Am. Chem. Soc.* **2005**, *127*, 12677–12683.

[9] a) P. R. Selvakannan, S. Mandal, S. Phadtare, R. Pasricha, M. Sastry, *Langmuir* **2003**, *19*, 3545–3549; b) H. Joshi, P. S. Shirude, V. Bansal, K. N. Ganesh, M. Sastry, *J. Phys. Chem. B* **2004**, *108*, 11535–11540.

[10] a) W. Xie, P. Xu, Q. Liu, *Bioorg. Med. Chem. Lett.* **2001**, *11*, 1699–1701; b) L. Chen, Y. Du, X. Zeng, *Carbohydr. Res.* **2003**, *338*, 333–340.

[11] a) E. H. Sargent, *Adv. Mater.* **2005**, *17*, 515–522; b) W. W. Yu, X. Peng, *Angew. Chem.* **2002**, *114*, 2474–2477; *Angew. Chem. Int. Ed.* **2002**, *41*, 2368–2371; c) X. Zhao, I. Gorelikov, S. Musikhin, S. Cauchi, V. Sukhovatkin, E. H. Sargent, E. Kumacheva, *Langmuir* **2005**, *21*, 1086–1090.

[12] a) E. Hutter, J. H. Fendler, *Adv. Mater.* **2004**, *16*, 1685–1706; b) C. F. Bohren, D. R. Huffman, *Absorption and Scattering of Light by Small Particles*; John Wiley & Sons: New York, **1998**.

[13] J. Fink, C. J. Kiely, D. Bethell, D. J. Schiffrin, *Chem. Mater.* **1998**, *10*, 922–926.

[14] S. H. Chen, K. Kimura, *Langmuir*, **1999**, *15*, 1075–1082.

[15] a) R. H. Terrill, R. H. Terrill, T. A. Postlethwaite, C. Chen, C. Poon, A. Terzis, A. Chen, J. E. Hutchison, M. R. Clark, G. Wignall, J. D. Londono, R. Superfine, M. Falvo, C. S. Johnson, E. T. Samulski, R. W. Murray, *J. Am. Chem. Soc.* **1995**, *117*, 12537–12548; b) A. Badia, S. Singh, L. Demers, L. Cuccia, G. R. Brown, R. B. Lennox, *Chem. Eur. J.* **1996**, *2*, 359–363.

[16] H. J. Zhang, Y. Ding, C. Zhang, J. Shen, *Chin. J. Nat. Med.* **2004**, *2*, 354–358.

[17] Y. Ding, X. H. Xia, C. Zhang, *Nanotechnology* **2006**, *17*, 4156–4162.

Received: July 15, 2006
Published online: January 19, 2007

